Cardiac afferent activity modulates early neural signature of error detection during skilled performance

Abbreviated title: Cardiac influences on early error monitoring

Gabriela Bury[2], Marta García Huesca[3], Joydeep Bhattacharya[1], María Herrojo Ruiz*[1]

[1] Department of Psychology, Goldsmiths University of London, London, UK

[2] The Ear Institute, University College London, London, UK

[3] Biological and Health Psychology Department, Autonoma University Madrid, Madrid, Spain

Corresponding author: María Herrojo Ruiz, email: M.Herrojo-Ruiz@gold.ac.uk. Address: Department of Psychology, Goldsmiths, University of London. Lewisham Way, New Cross, London SE14 6NW (UK).

Abstract

Behavioral adaptations during performance rely on predicting and evaluating the consequences of our actions through action monitoring. Previous studies revealed that proprioceptive and exteroceptive signals contribute to error-monitoring processes, which are implemented in the posterior medial frontal cortex. Interestingly, errors trigger changes in autonomic nervous system activity such as pupil dilation or heartbeat deceleration. Yet, the contribution of implicit interoceptive signals of bodily states to error-monitoring during ongoing performance has been overlooked. This is more surprising given the evidence on the relevance of interoceptive signals for the modulation of perceptual, affective and cognitive processes.

We investigated whether cardiovascular interoceptive signals influence the neural correlates of error processing during performance, with an emphasis on the early stages of error processing. We recorded participants' electroencephalography and electrocardiogram during the performance of highly-trained music pieces in musicians. Previous event-related potential (ERP) studies revealed that pitch errors during skilled musical performance are preceded by an error detection signal, the pre-error-negativity (preERN), and followed by a later error positivity (PE). In this study, by combining ERP, source localization and multivariate pattern classification analysis, we found that the error-correct ERP waveform had a larger amplitude within 40-100 ms following errors in the systolic period of the cardiac cycle. This component could be decoded from single-trials, was

dissociated from the preERN and PE, and stemmed from the inferior parietal cortex, which is a region implicated in cardiac autonomic regulation. In addition, the cardiac phase influenced behavioral alterations resulting from errors, with a smaller post-error slowing and less perturbed velocity in keystrokes following pitch errors in the systole phase of the cardiac cycle. This study provides the first evidence of preconscious visceral information modulating neural and behavioral responses related to early error monitoring during skilled performance.

Introduction

Detection and evaluation of errors is central to the acquisition of complex motor skills, such as those needed in dance or music performance (Wolpert and Kawato, 1998; Palmer, 2006). Over the last decades, the error-monitoring processes have received broad attention in the neuroscientific community. Studies of event-related brain potentials (ERPs) have revealed a neural response peaking at 80-100 ms after error commission, termed error-related negativity (ERN, Gehring et al, 1993), and followed by a later error positivity (PE, Falkenstein et al, 2000). The ERN is considered to reflect an early prediction error signal and is localized in the posterior medial frontal cortex (pMFC), anterior cingulate cortex (ACC), and pre/suplementary motor area (pre-/SMA) (Kiehl et al., 2000; Miltner et al. 2003; Bonini et al., 2014). Following extensive training, for instance during skilled musical performance, early error detection in the pMFC/ACC precedes error commission by 50-100ms (pre-error-negativity, preERN; Maidhof et al., 2009, Ruiz et al., 2009). Importantly, such an early latency of the preERN has been found in tasks with different performance tempi (Maidhof et al., 2009; Ruiz et al., 2009, 2011; Palmer et al., 2012; Strübing et al., 2012).

Oscillatory analyses of the preERN support the finding that primarily changes in theta (4-7 Hz) and beta (13-30 Hz) oscillations in the pMFC contribute to the ERP modulation (Ruiz et al., 2011). In addition to early error detection in the pFMC, this study reported an increase in coupling through beta oscillations (13-30 Hz) between the pFMC and the lateral prefrontal cortex (lPFC) in anticipation of the error. Larger beta-band coupling between the pFMC and lPFC was associated with larger corrective adjustments at the pitch error, in form of reduced keystroke velocity. This finding is in line with the suggested role for the lPFC in the implementation of behavioral adjustments following error commission in reaction-time tasks (Miller, 2000; Wittfoth et al., 2009; Cavanagh et al., 2009).

The latter PE component consists of an earlier frontocentral and a later centroparietal deflection, which peak at 200 and 300 ms following errors, respectively. The late PE component, in particular, reflects an accumulation of evidence or decision confidence that an error occurred (Orr and Carrasco, 2010; Boldt and Yeung, 2015). Interestingly, PE is generated in the rostral ACC and the insular cortex (Herrmann et al., 2004; Dhar et al., 2011). Thus, the neural signatures of error

detection and evaluation rely on an extended cortico-subcortical network beyond the pMFC (Ullsperger et al., 2014).

The involvement of the anterior insula – a key region for interoceptive processing (Craig, 2009; Barrett and Simmons, 2015) – during error processing aligns with the reported changes in the ongoing autonomic nervous system, such as heartbeat deceleration and enhanced pupil dilation, following errors (Hajcak et al., 2003; Wessel et al., 2011, Bastin et al., 2017). Further, the ventral part of the ACC is a key recipient of visceral information from the internal organs (Stevens et al., 2011; Critchley and Harrison, 2013). The findings by Hajcak and colleagues (2013) indicate that error commission may be associated with interoceptive processing, yet we still do not fully understand how the interoceptive signals of bodily states contribute to error-monitoring during ongoing performance. This is more surprising given the increasing evidence on the relevance of interoceptive information for the modulation of perceptual, affective and cognitive processes (Critchey and Harrison, 2013; Park et al., 2014). Recent work has shown that changes in interoceptive states (heart rate deceleration) following incorrect responses might provide internal feedback about performance accuracy (Lukowska et al., 2018). Also following errors, the skin-conductance response – a measure of the autonomic nervous system – correlates with the PE amplitude and the degree of post-error slowing (Hacjak et al., 2003). What remains unclear is whether interoceptive cues influence error-monitoring processes during earlier stages of error detection. New theoretical accounts suggest that interoceptive processing is not limited to monitoring the physiological state of the body but is also crucially involved in generating future predictions about bodily states (Barrett and Simons, 2015). Accordingly, early interoceptive cues could shape ongoing error-monitoring to influence the predicted future bodily states associated with error commission.

The present study tested the hypothesis that early detection of errors during skilled performance is influenced by implicit cardiovascular interoceptive information. We recorded electroencephalography (EEG) and electrocardiogram (ECG) of skilled pianists during performance of highly-trained musical excerpts. There are two dominant approaches to study brain-body communication during cognition. First, analysis of the heartbeat-evoked potential (HEP)

– neural responses locked to heartbeats – has been used to demonstrate a role of visceral information in bodily consciousness, conscious perception and emotional processing (Pollatos and Schandry 2004; Luft and Bhattacharya, 2015; Babo-Rebelo et al., 2016a and 2016b; Park et al., 2016). This approach is typically followed in studies that do not measure concurrent motor responses, which could overlap with the HEP modulation. Second, the timing of ongoing fluctuations in the cardiac cycle with respect to an event, that is, whether the event coincides with the cardiac systole or diastole, is shown to exert an influence on perceptual and sensory processing (Garfinkel et al., 2014; Azevedo et al., 2017; Al et al., 2018). This second approach has also long demonstrated that the cardiac phase can have an effect on task performance, either through a modulation of motor preparation or sensory processing (in stimulus-response paradigms; Weisz and Adam, 1996; Edwards et al., 2007). For example, response to a stimulus presented during the cardiac systole can be slower, possibly due to an increase in blood pressure when the arterial baroreceptors are naturally stimulated by the arrival of the pulse pressure wave during systole (Edwards et al., 2007).

Here, we adopted this second approach and undertook a cardiac-cycle fluctuation-based analysis to assess whether the alignment of performance errors to different phases of the cardiac cycle biases neural and behavioral responses during error processing. Neural responses to pitch errors during performance were analyzed in terms of ERP, source localization and multivariate pattern classification techniques and dissociated between different phases (systole, diastole) of the cardiac cycle.

In addition to the cardiac-cycle fluctuation-based analysis, we further aimed to replicate the previous results of the preERN and PE preceding and following pitch errors, as well as the behavioral effects surrounding errors (pre- and post-error slowing and reduced keystroke velocity in pitch errors, Ruiz et al., 2009; Maidhof et al., 2009; Palmer et al., 2012). This additional goal was motivated by the recent call for replication of small scale neuroimaging studies (Button et al., 2013; Open Science Collaboration, 2015).

Materials and Methods

Participants

Sample size considerations were based on prior data from our study using this paradigm (Ruiz et al., 2009), which we used to estimate the minimum sample size for a statistical power of 0.95, with an alpha of 0.05, using the MATLAB function sampsizepwr (https://de.mathworks.com/help/stats/sampsizepwr.html). Using the preERN and PE data from the 19 pianists that participated in that study, we obtained a minimum sample size of 17 (preERN) and 11 (PE), respectively. In addition, the non-parametric effect sizes of the previously reported preERN and PE were 0.875 and 0.812, respectively (non-parametric effect size estimator, Grissom and Kim; 2012).

Eighteen right-handed healthy pianists (10 females; mean age = 26.6, s.d. = 2.7 years) participated in the present study. They were professional pianists or students at a London music conservatoire, and had self-reported normal hearing. All participants gave written informed consent, and the study protocol was approved by the local ethics committee at the Department of Psychology, Goldsmiths, University of London. Participants received a monetary remuneration for participating in the study and memorising the musical material prior to their participation. One participant was excluded from the analysis due to poor quality of the EEG signal, leaving 17 participants for the analysis.

Stimulus Materials

Stimuli were four musical sequences selected after Ruiz et al, (2009). In brief, the sequences were right-hand excerpts of Preludes V and VI of the Well-Tempered Clavier by J. S. Bach. These pieces were chosen because of their homogeneity in terms of the duration of notes (sixtinth notes) and regular (isochronous) time interval between consecutive notes. The length of these excerpts was 200, 201, 202 and 185 notes, respectively. As in Ruiz et al. (2009), participants were instructed to perform at a fast tempo (inter onset interval, IOI = 125ms) to induce errors. The duration of each piece was around 25 s. Participants were instructed to rehearse and memorize the pieces at the correct tempo and without finger-tracking before coming to the experimental session. Prior to EEG and MIDI recording, we verified that pianists managed to play all pieces from memory without looking at their hands.

Experimental Design

Participants were seated comfortably on an adjustable piano stool in front of a digital piano (Yamaha Digital Piano P-255, London, United Kingdom) in a light-dimmed room. They were instructed, via a PC monitor, to perform each piece from beginning to end without stopping to correct errors, and to avoid visually tracking their finger movements by fixating on a central cross displayed on the PC monitor. The emphasis was placed on maintaining an accurate timing and playing the correct notes. All participants were naïve to the purpose of the study.

The experiment consisted of 60 trials, separated into two 30-trial blocks of approximately 20 min each. There were two practice trials at the beginning of each block for familiarization. We used a synchronization-continuation paradigm with the following timeline for each trial. Participants pressed a designated key with their left-hand index when ready to begin a trial. A silent time-interval of 500 ms was followed by the visual presentation of the first two bars of the music score for 4000 ms, indicating which of the four excerpts, randomly selected, had to be played. After 2500 ms of the visual cue (score), a metronome started pacing the tempo corresponding to the piece: four metronome beats for scores at 120 bpm (2000 ms), five metronome beats for ones at 160 bpm (1875 ms). Participants had to internally entrain their timing to the metronome clicks and get ready to start playing after the metronome beats and visual cue disappeared. Participants were instructed to start playing only when they saw a green ellipse on the monitor (shown 50 ms after the visual and auditory cues vanished) and stop playing when the ellipse turned red (approximately after 27 s).

EEG, ECG and MIDI recording

EEG and ECG signals were recorded using a 64-channel (extended international 10–20 system) EEG system (ActiveTwo, BioSemi Inc.) placed in an electromagnetically shielded room. During the recording, the data was high-pass filtered at 0.16 Hz. The vertical and horizontal eye-movements (EOG) were monitored by electrodes placed above and below the right eye and from the outer canthi of both eyes, respectively. Additional external electrodes were placed on both left and right mastoids as reference. The ECG was recorded using two external channels with a bipolar ECG lead II configuration (the negative electrode was placed on the chest bellow the right collar bone, and the positive electrode was placed on the left leg above the hip bone). The sampling frequency

was 512 Hz. Onsets of visual stimuli, key presses and metronome beats were automatically documented with markers in the EEG file. Performance was additionally recorded as MIDI files using the software Visual Basic and a standard MIDI sequencer program on a PC.

EEG Data Preprocessing

We used MATLAB (The MathWorks, Inc., MA, USA) and the FieldTrip toolbox (Oostenveld et al. 2011) for visualization, filtering and independent component analysis (ICA; runica). The EEG data were highpass-filtered at 0.5 Hz (Hamming windowed sinc FIR filter, 3380 points) and notch-filtered at 50 Hz (847 point). ICA was used to identify artifact componets related to eye blinks, eye movements and, crucially, the cardiac-field artifact (CFA). Inspection of the IC components to find the CFA was performed using the procedure suggested in the Fieldtrip toolbox (http://www.fieldtriptoolbox.org/example/use_independent_component_analysis_ica_to_remove_ecg_artifacts).

Following this approach, the time and the frequency data of the ECG signal were used to detect the QRS-complex and to correlate its time course with the IC time series. We typically found one or two ICs related to the CFA, which were subsequently removed. After IC inspection, we used the EEGLAB toolbox (Delorme and Makeig, 2004) to interpolate missing or noisy channels using spherical interpolation. Next, we transformed the data into common average reference.

In the analysis of epoched data (see *Event-related analysis and Heart-evoked responses* sections), we performed a final inspection of the epoched data with the EEGLAB toolbox and applied an automated rejection of noisy epochs using a voltage threshold of ±100 μV.

ECG data Preprocessing

The analysis of the ECG signal with Fieldtrip rendered the time course of the heartbeat and associated QRS complex. We then dissociated between different types of R-peaks, depending on the temporal difference between the R-peak and the subsequent keystroke (pitch error or correct note). Specifically, we selected R-peaks which were followed by a keystroke either (i) within 50-350 ms, corresponding to the systolic period of the cardiac cycle and the and the T waveform of the QRS complex (peaking at 233 [standard error of the mean or s.e.m. 8] ms after the R-peak on average); or (ii) between 400 ms and the beginning of the next R-peak (693 [15] ms on average),

corresponding to the diastole phase of the cardiac cycle (Figure 1). The systolic period, in which the blood is pumped out of the heart, is the window of maximal representation of baroreceptor afferent activity (Fadel et al., 2003) and when cardiac cycles effects on perception and cognition are typically observed (Motyka et al., 2007; Gray et al., 2012; Garfinkel et al., 2014). The diastole is the remaining period of the cardiac cycle during which afferent activity is quiet. From hereafter, events (e.g. keystrokes) in each of these periods of the cardiac cycle will be labelled as pertaining to bin1 (systole) or bin2 (diastole), respectively.

Performance analysis and performance-related modulation of the heartbeat

After Ruiz et al., (2009), we analyzed the MIDI files to detect pitch errors during piano performance. In addition, we extracted information corresponding to the timing of note onsets, the inter-onset-interval (IOI, ms), i.e. the time between consecutive keystrokes, and the keystroke velocity, related to the loudness. As in our previous studies (Ruiz et al. 2009, 2011), we exclusively selected "isolated" pitch errors and correct notes as events for the EEG analysis. Isolated pitch errors and correct notes refer to events surrounded by correct pitch notes for at least two preceding and following keystrokes. General performance was assessed in terms of average timing (mean IOI, mIOI, in ms), temporal variability (coefficient of variation of IOI, cvIOI), average MIDI keystroke velocity (mKvel, related to loudness), and error rates.

To assess changes in the heart rate preceding and following error commission (e.g. Bastin et al., 2017), relative to performance of correct note onsets, we used the time series of R-peaks and inter-beat intervals (RR-interval, ms).

Event-related potentials: Keystroke-locked preERN and PE analysis

Before analysing the influence of cardiac interoceptive signals on error-processing, we first tried to replicate previous results reporting the emergence of a preERN ([-80, -30] ms) and PE ([150, 250] ms) ERP components triggered by pitch errors during piano performance (Ruiz et al., 2009; Maidhof et al., 2009). To that aim, analysis of keystroke-locked data focused on isolated pitch error and correct note events (see previous section). Epochs were extracted within [-1000, 1000] ms around the keystroke. After EEG preprocessing and artifact removal, the average number (s.e.m.) of trials available for this analysis was 170 (15) errors and 1600 (200) correct notes. Because pitch

errors are typically slower than correct key presses, and the difference in latencies could lead to a modulation of the ERP waveforms (see Maidhof et al. 2013), we performed a control analysis by selecting a subset of the pitch error events with comparable timing to that of isolated correct events. Specifically, for each subject, we selected pitch error events with an IOI falling within the subject-specific range of IOIs for isolated correct events. This resulted in a group-average of 73 (9) pitch error trials available (no difference in IOI between this subset of error trials and correct events, 126 (1) ms and 125 (0.1) ms, respectively, $p = 0.3250$). After we controlled for temporal differences between types of events, this analysis replicated the previous ERP findings (see below). Accordingly, the main analyses throughout the manuscript focused on the total set of pitch error trials as a larger number of trials was thought to improve the signal-to-noise ratio.

The analysis (see *Statistical Analysis*) was carried out within [-200, 300] ms as this interval contains the previously reported preERN ([-80, -30] ms) and PE ([150, 250] ms) as well as a potential effect preceding the pre-error keystroke (Maidhof et al., 2013). The ERP data were corrected with a baseline reference level from -300 to -150 ms prior to the keystroke (Ruiz et al., 2009).

The ERP waveforms were additionally assessed by comparing trials in which the keystroke coincided with the systolic (bin1) or diastolic (bin2) phase of the cardiac cycle.

Source Reconstruction

Between-conditions differences at the source level were assessed using L2-norm minimum-norm estimates (MNEs, Hämäläinen and Ilmoniemi, 1994; Dale et al., 2000) and a standard brain T1-weighted MRI template (Colin27 brain in MNI152 space). MRI segmentation was performed with a FieldTrip pipeline (http://www.fieldtriptoolbox.org/workshop/ohbm2018) to generate a volumetric mesh as a head model with five compartments: scalp, skull, cerebrospinal fluid (csf), gray and white matter. Co-registration of the MRI and EEG coordinate system was then carried out using the anterior and posterior commissure as the anatomical landmarks. Next, the FieldTrip-SimBio pipeline was implemented to calculate EEG forward solutions using the finite element method (FEM; Vorwerk et al., 2018). Next, inverse solutions were computed using the L2-norm MNE method, as implemented in the “FieldTrip” software (minimum-norm estimate, based on Dale et al.,

2000; Lin et al., 2004). MNE sources were estimated for each grid point in the window of the significant ERP effect, the individual source solutions were interpolated to a template MNI mesh. The noise-covariance matrix was estimated for each participant using a time window preceding he central error and correct events, within [-0.7, -0.3] s. Scaling of the noise-covariance matrix was performed with regularization parameter $\lambda = 0.1$.

Multivariate Pattern Classification Analysis (MVPA)

We first used MVPA (Duda et al., 2000; Haxby et al., 2001) to assess whether error and correct trials could be classified using the heart rate (HR) information from the three preceding interbeat intervals (three features).

In addition, for the EEG analysis, MVPA was used to determine whether the phase of the cardiac cycle (systole vs diastole) could be decoded from the neural responses to errors on a trial-by-trial basis (Duda et al., 2000; Haxby et al., 2001). In this analysis we used a subset of the data from each participant, to match the number of error trials from systolic and diastolic phases. The features selected for MVPA were the ERP amplitude values in the set of 64 electrodes. MVPA was performed in the range [-150, 300] ms – similar to the interval used for the standard ERP analysis. Each data epoch was normalized using this interval (full-epoch-length normalization: Grandchamp and Delorme, 2011). The range -150 to 300ms was divided into 50 adjacent windows of 10-ms width.

For the HR-MVPA, a support vector machine (SVM, a MATLAB library by Chang and Lin, 2011) with a radial basis kernel function was trained to distinguish between error and correct trials. For the EEG-MVPA, however, a SVM with a radial basis kernel function was trained separately in each time window to distinguish between trial classes (keystroke in the systolic or diastolic period).

In all MVPA cases, we used 10-fold leave-one-out cross-validation to estimate the validity of the SVM model. A participant-based classification was performed first, and subsequently, we estimated the population decoding accuracy by averaging across participants.

Statistical Analysis

Statistical analysis of group-level behavioral data was performed using pair-wise permutation tests (Good, 2005), using the difference between condition means as the test statistic. Whenever multiple comparisons were performed, we applied an adaptive two-stage linear step-up procedure to control the false discovery rate (FDR) at level $q = 0.05$ (Benjamini et al., 2006; termed $p < 0.05$, FDR-corrected hereafter).

The group-level statistical inference on the difference between error and correct trials in keystroke-locked ERPs was conducted using permutation tests with a cluster-based threshold correction to control the family-wise error (FWE) at level 0.05 (dependent samples *t*-test, 1000 iterations; Maris and Oostenveld, 2007). Experimental cluster-based test statistics being in the 2.5^{th} and 97.5^{th} percentiles of the permutation distribution were considered significant (two-tailed test, $p < 0.025$). Using this procedure, the assessment of statistical differences in the keystroke-locked ERP was performed within [-100 ms, 300 ms]. To assess the influence of cardiac information on neural responses we compared the keytroke-locked error-correct ERPs between bin1 (systole) and bin2 (diastole) epochs. Statistical analysis for this comparison was also performed within [-100, 300] ms.

The statistical analysis was complemented with a nonparametric effect size estimator, the probability of superiority for dependent samples or PS_{dep} (Grissom and Kim; 2012). PS_{dep} is an estimation of the probability (maximum 1) that in a randomly sampled pair of matched values *i* (from same individual), the value from Condition B will be greater than the value from Condition A: $PS_{dep} = Pr\ (XB_i > XA_i)$. Throughout the paper, this index will be provided in association with each pairwise permutation test (excluding the cluster-permutation test on spatiotemporal features, for which PS_{dep} is not defined).

Differences between conditions in source reconstruction were also assessed at the group level using the cluster-based permutation test (Maris and Oostenveld, 2007) As in the case of statistics at the channel level, correction for multiple comparisons at the source level was performed by controlling the FWE at level 0.05 (and alpha level 0.025, two-tailed test).

Finally, for the MVPA, we first tested whether the classification accuracy in each participant was significant at the participant level. To that aim, the null distribution of accuracy in each participant was estimated by performing the MVPA 500 times after randomly shuffling the class labels in the data. At each time window (EEG-MVPA) or at once (HR-MVPA) we calculated the *p*-values as the frequencies of permutation accuracies that are greater than or equal to the experimental decoding accuracy. Note that this approach to assessing statistical significance on the subject level (see also Ruiz et al., 2014) is preferred than comparing empirical classification accuracies against a theoretical chance level of 50% for two-class classification. The reason is that the empirical chance level in two-class classification problems prominently deviates from 50% for small sample sizes (small number of trials; Combrisson and Jerbi, 2015).

For the EEG-MVPA, the single-subject MVPA thus aimed to complement the cardiac cycle-based ERP group results by revealing in individual participants the effect of the phase of the cardiac cycle on the modulation of neural responses to errors. Next, statistical assessment with a permutation test was performed on the group level to localize the time windows showing an effect of above-chance decoding accuracy across the pianist population. The population chance level used in this analysis was the mean across individual permutation-based chance levels, extracted as the mean of the null distribution of decoding accuracies in each participant. Of note, however, for MVPA single-subject statistical assessment might be preferred over group-level statistical analysis when using the mean accuracy as test statistic, as statistical inference on the group level using this test statistic is not optimal to describe whether effects related to information content are how “typical” in the population (that is, whether they are present in the majority of the population; Allefeld et al., 2016).

Results

Behavioral Results

The details of the behavioral data are shown in Table 1. All data are provided as mean and s.e.m. Our participants played the musical excerpts at the instructed tempo (average time between

consecutive notes, or IOI, was 125 [s.e.m. 0.1] ms), when excluding pitch errors in the analysis. The percentage of isolated pitch errors was 1.4% (0.2%), and the percentage of total pitch errors was 3.7% (1%). Pitch errors were distributed across all positions of each excerpt, indicating that they were not linked to an isolated part of the sequence. In terms of timing, pitch errors had a slower tempo (larger IOI relative to previous keystroke) than correct key presses ($p = 0.002$, $p < 0.05$, FDR-corrected, $PS_{dep} = 1$; Table 1). With regard to MIDI velocity, pitch errors had a significantly smaller value than correct key presses (64 [1] and 66 [1], respectively, $p = 0.006$, $p < 0.05$, FDR-corrected, $PS_{dep} = 0.76$).

Timing and keystroke velocity data at keystrokes surrounding pitch errors were consistent with post-error adaptation effects but also with pre-error alterations in performance. Specifically, pitch errors were followed by significantly slower (delayed) keystrokes in the subsequent +K, +2K, +3K, +4K, +5K and +6K events and preceded by a slower keystroke at -K relative to correct events at those same positions ($p < 0.05$, FDR-corrected in all cases; PS_{dep} in the range 0.73-0.94; non-significant difference at -2K and +7K, $p > 0.05$; Figure 2). The slowing of IOI following pitch errors relative to correct key presses was, however, less pronounced than the slowing of IOI at the errors ($p < 0.05$, FDR-corrected in all cases +K to +6K; PS_{dep} in the range 0.71-0.87). A significantly reduced MIDI velocity was also observed at the previous and subsequent keystrokes relative to the correct notes in those positions (65 [1] at -K and +K relative to errors; 66 [1] at events surrounding cortect note onsets, $p < 0.05$, FDR-corrected, PS_{dep} 0.94 and 0.59, respectively). Consequently, behavioral alterations in performance were most pronounced at pitch errors, yet extended to the keystroke preceding as well as several keystrokes following pitch errors.

The subset of pitch errors selected to match correct events in timing (IOI, ms; see Methods), which were subsequently used in a control ERP analysis, exhibited significant post-error slowing effects. Specifically, the mean IOI of the keystrokes following the pitch error at +K, +2K and +3K positions was 136 (4) ms, 137 (5) ms, and 137 (4) ms, respectively, thus being larger than the average IOI, 126 (1) ms, of the subset of pitch errors ($p < 0.05$, FDR-corrected). The keystroke velocity was also reduced at position +K following the pitch error (65 [1], which was smaller than in correct events: $p < 0.05$, FDR-corrected). Therefore, the general effects of post-error slowing in tempo and reduced

loudness were maintained after we controlled for the timing of the pitch errors to match the values of the correct events.

Effects of behavioral performance on the heart rate

On average, the cardiac interbeat interval during performance was 693 (15) ms. Using as reference R-peak the one immediately preceding the wrong keystroke (R_0), we assessed changes in the heart rate at preceding (R_{-3}, R_{-2}, R_{-1}) and following (R_1, R_2) R-peak positions. A similar analysis was performed for R-peaks surrounding correct keystrokes (Figure 1C). Before and after correct events, there was a general linear increase (slowing) of the RR both before and following the keystroke ($p < 0.05$, FDR-corrected, PS_{dep} in range 0.76 – 0.88). For pitch errors, we found that the interbeat interval immediately preceding errors was larger than the previous RR-interval (RR_0 = 0.691 [0.008] ms, RR_{-1} = 0.689 [0.009] ms, $p < 0.05$, FDR-corrected, PS_{dep} = 0.76) but not significantly different from the post-error interbeat intervals. A comparison between the RR-interval of error and correct events demonstrated larger values following correct keystrokes at position +2 ($p < 0.05$, FDR-corrected, PS_{dep} in range 0.92). Additionally, we assessed the relative change between consecutive RR-intervals (RR-interval at n position relative to RR-interval at the preceding n-1 position), to test for error-correct differences in interbeat changes independently of the general linear increase of RR-intervals found for correct trials (Figure 1D). This representation demonstrated a relatively small RR-interval change at -2 and -1 RR positions in error trials, as compared to the larger changes found in correct trials ($p < 0.05$, FDR-corrected, PS_{dep} in range 0.64 – 0.82). Immediately before error keystrokes, however, this pattern was altered as there was a sudden increase in the RR-interval relative to the earlier RR-intervals (significant change increase in error trials at position 0, just before the error keystroke: $p < 0.05$, FDR-corrected, PS_{dep} in range 0.84). Following correct and error key presses, there was a reduction in the RR-interval change relative to the change found at position 0, which can be observed as a negative change in Figure 1F ($p < 0.05$, FDR-corrected, PS_{dep} in range 0.76 – 0.85).

Thus, we found that pitch errors were associated with a generally faster HR, yet were preceded by a slowing down of the RR-interval immediately preceding the key press. Pitch errors were then followed by a larger heart rate (HR) acceleration relative to correct keystrokes.

MVPA performed using trial-based patterns containing the three RR-intervals preceding the keystroke (error, correct) demonstrated a significant classification accuracy on the single-participant level in 13/17 participants ($p < 0.05$) and a significant group-level population accuracy of 57% ($p = 0.004$). A similar analysis including additionally the RR-interval following the error and correct key presses demonstrated a drop in the prevalence of the effect, as the classification accuracy on the single-participant level was significant in only in six pianists ($p < 0.05$).

Thus, information about an upcoming error or correct key press was more consistently decoded from the HR patterns preceding the keystroke.

Effects of the cardiac cycle on behavioral performance

Pitch errors during the diastolic phase (bin2) as compared to those in the systolic phase (bin1) led to a significantly larger post-error slowing and reduced keystroke velocity at +2K ($p < 0.05$, FDR-corrected; Post-error slowing, mean IOI at +2K: 137 (6) ms in bin1 and 144 (9) ms in bin2, $PS_{dep} = 0.69$; Keystroke velocity: 66 (1) in bin1 and 65(1) in bin 2, $PS_{dep} = 0.71$). These effects were not found in the immediate keystroke following pitch errors (+K) or at +3K ($p > 0.05$). Further, when assessing correct note events, we found no significant dissociation between the performance data in bin1 and bin2. These findings support that the effect of the phase of the cardiac cycle on performance was limited to timing and loudness properties of error processing in the subsequent keystroke at position +2K.

Changes in the RR-interval following errors did not differ when separately assessing error key presses in the cardiac systole or diastole ($p > 0.05$).

Keystroke-locked ERP Analysis

The difference between the ERP waveforms for error and correct trials was statistically assessed with cluster-based permutation tests within [-100, 300] ms. We found a significant negative cluster preceding and a positive cluster following pitch errors ($p = 0.0159$ and 0.0199, respectively, $p < 0.025$, two-sided test). The negative cluster was due to a less positive pre-keystroke waveform in error trials than in correct trials within [-70, -30] ms (Figure 3A) with a frontal topography (Figure

3B). The positive cluster had a frontocentral topography and was related to a positive post-keystroke deflection within [80, 300] ms in error trials (Figure 3C), which was not observed in correct trials (Figure 3D).

Figure 3E displays the significant source localization outputs using minimum-norm estimates. In the time window of the preERN, there was a significantly smaller activation ($p < 0.025$, FWE-corrected) in a set of regions of the pMFC, such as the SMA (Brodmann area, BA 6, peak MNI coordinate at [X,Y,Z] = [9, 17, 68] mm), the ACC (BA 32 at [-4, 17, 38] mm), but also in the mPFC (BA 9 at [-12, 37, 23] mm). In the PE time window, significant differences in minimum-norm estimates were found in the ACC (BA 24 at [-7, 29, 18] mm) and the mPFC (BA 9 at [-10, 50, 48] mm; $p < 0.025$, FWE-corrected).

To exclude the potential confounding factor of different latencies in error trials driving the modulation of the preERN, as a control analysis we contrasted correct trials to a subset of error trials with matched latencies to the correct trials (see behavioral results: matched IOI with respect to the preceding keystroke). A cluster-based permutation test demonstrated a significant negative ERP deflection at -180 ms and a significant PE following errors around 150-350ms (Figure S1). A second frontocentral negative cluster was found, corresponding to the preERN, but showed a trend toward significance ($p = 0.035$). Thus, when differences in latencies preceding the error and correct keystrokes were controlled for, early error detection was associated with a negative deflection already 180 ms before the wrong keystroke and the preERN (trend) around [-80,-50] ms. As suggested by the main analysis, the PE was elicited following errors..

ERP analysis locked to keystrokes in different phases of the cardiac cycle

We evaluated the keystroke-locked error-correct difference ERP waveform separately for trials corresponding to bin1,2 (systole, diastole). This analysis is similar to the one performed in the keystroked-locked ERP section (and Figure 3), but with a split of epochs according to the temporal interval (systole, diastole) in which the key following the R-peak was struck. A cluster-based permutation test performed within [-100, 300] ms revealed a significant negative difference

between the error-correct ERP waveform in systolic and diastolic phases of the cardiac cycle ($p < 0.025$, Figure 4). The effect reflected a more positive error-correct ERP modulation for systole trials around 40-100 ms in a cluster of left centro-posterior electrodes. Based on the latency and topography, this effect seems to be dissociated from the error-related ERP components preERN and PE (Figure 3).

Of note was also that the time interval preceding the error events in bin1 and bin2 was not significantly different (the IOI relative to the previous keystroke was 147 [9] ms and 148 [7] ms in bins 1 and 2, respectively: $p > 0.05$). Thus, errors in the systolic or diastolic cardiac phase had similar temporal properties with respect to the previous keystroke, and they led to differences in the subsequent behavioral alterations later at +2K, that is, around 280 (10) ms following key presses (See *Effects of the cardiac cycle on behavioral performance*). Accordingly, the significant ERP effect within 40-100ms cannot be accounted for by a cardiac phase effect on the temporal properties of key presses within that temporal interval.

Source localization analysis demonstrated a significant difference between the systolic and diastolic modulation of the error-correct ERP, with significantly increased cortical activation in the left inferior parietal cortex for systole trials (left BA 39 at [-30, -75, 40] mm).

Multivariate Pattern Classification Analysis of ERP waveforms

Next, we used MVPA to assess whether the difference between the two phases of the cardiac cycle could be decoded from the patterns of single-trial ERP waveforms locked to pitch errors. For this analysis single epochs were locked to pitch error keystrokes falling either within the systolic (bin1) or diastolic (bin2) phase of the cardiac cycle. MVPA was evaluated at each time bin using as features the ERP amplitude values in the set of 64 channels.

Significant above-chance classification accuracy was found on the participant level preceding and following the pitch error in 15/17 participants ($p < 0.05$, FDR-corrected in all cases after control of FDR. Figure 5). On the group level, MVPA revealed a significant above-chance classification accuracy within [-86, -66] ms, [53, 73] ms and later within [173, 213] ms ($p < 0.05$, FDR-corrected, $PS_{dep} = 0.970$). Note that the second window converges with the cardiac cycle-based ERP effect

reported in the previous section (*ERP analysis locked to keystrokes in different phases of the cardiac cycle*). These results indicate that the patterns of EEG activity across the cluster-related electrodes encoded class-related information, i.e. distinguishing between erroneous keystrokes coinciding with the systolic or diastolic phase of the cardiac cycle. A similar analysis performed with correct trials rendered no significant decoding accuracy at the group level ($p > 0.05$, mean accuracy 50%), but a significant single-participant decoding accuracy in 12 /17 subjects around -100 ms prior to the keystroke and after 200 ms ($p < 0.05$, FDR-corrected in all cases after control of FDR). Thus, the multivariate patterns of ERP waveforms were discriminative of the phase of the cardiac cycle more consistently for error trials. Moreover, primarily in error trials was there a result of significant decoding accuracy after 0 ms and before 100 ms, a time window that encompasses the early error-correct ERP modulation for systole versus diastole. Errors in the systolic or diastolic phase had similar temporal properties with respect to the previous keystroke and at the following event at +K, yet they differed at +2K. Accordingly, the MVPA results obtained in the time windows preceding ([-86, -66] ms) and following ([53, 73] ms) the keystroke cannot be accounted for by timing differences in the two classes of error events.

Additional Control Analyses

To control for the possibility that differences in the ERP waveforms in each cardiac phase bin were accounted for by differences in the concurrent ECG modulations, we tested for statistical differences between the ECG signal locked to keystroke events in bin1 and bin2; Figure 1D-E). In correct trials, the keystroke-locked ECG differed significantly between bin1 and bin2 within [-53, -8] ms preceding the key press ($p < 0.05$, FDR-corrected; $PS_{dep} = 0.875$). In error trials, the shifted ECG waveforms also differed significantly between bin1 and bin2 trials in the pre-keystroke interval within [-74, -18] ms ($p < 0.05$, FDR-corrected; $PS_{dep} = 0.818$). Thus, differences between the ECG signals in bin1 and bin2 conditions cannot account for the post-keystroke effects found with the cluster-based permutation test around 40-100ms. Neither can these differences be the source of the post-keystroke MVPA results at [53, 73] ms. However the MVPA effects found preceding the keystroke could be influenced by the ECG differences and should be taken with care.

In sum, the different behavioral and ECG control analyses support that the results from the ERP and MVPA analysis for bin1 and bin2 events found in the post-keystroke interval within 40-100 ms

(ERP) and 53-73ms (MVPA) primarily reflect a cardiac-cycle-related influence on early error-monitoring processes.

Discussion

This study sought to determine the role of cardiac afferent information in modulating early stages of error-monitoring during highly trained performance. In addition, we aimed to replicate the emergence of an anticipatory error detection ERP, the preERN, and a later PE during error commission in this setting, as reported in previous studies (Maidhof et al., 2009; Ruiz et al., 2009). Our results revealed that fluctuations in the cardiac cycle influence neural responses related to an early stage of error processing during action monitoring. Precisely, we found that the error-correct ERP waveform had a more pronounced positive deflection within 40-100 ms for keystrokes that coincide with the systolic period of the cardiac cycle when compared with the cardiac diastole. This effect was dissociated in both time and topography from the specific error detection and evaluation components, the preERN and PE, respectively (Maidhof et al., 2009; Ruiz et al., 2009). Moreover, information about the systolic and diastolic phase of the cardiac cycle could be decoded from patterns of error-related neural activity on the single-trial and subject levels. In addition, we found that pitch errors in the systolic phase led to a smaller post-error slowing (PES) and less pronounced keystroke velocity reduction at position +2K. These findings support that during systole, when baroreceptor afferent activity is maximal, the neural responses to error processing are more pronounced, whereas the behavioral alterations following errors are attenuated.

The finding of an enhanced modulation of error-related neural responses during the cardiac systole is comparable to the previously reported effect of this cardiac phase on amplifying fear, pain and threat-related processing (Gray et al., 2012; Garfinkel et al., 2014). A vast number of studies have investigated the impact of the dynamics of baroreceptor afferent activity on neural and psychological processes (Motyka et al., 2007; Gray et al., 2011; Garfinkel et al., 2014; Fiacconi et al., 2016; Azevedo et al., 2017). Baroreceptors are mechanoreceptors located in the heart and major blood vessels, which encode fluctuations in the cardiac cycle, such as the timing and amplitude of each heartbeat (Fadel et al., 2003). At the cortical level, visceral afferent

representations – including those derived from baroreceptor activity – converge in the insular cortex, where they are integrated with pain and temperature sensations to guide behavior (Bennarroch, 2012; Critchley and Garfinkel, 2018). Previous studies have shown that during the cardiac systolic phase, there is a more pronounced processing of painful and fearful stimuli, threat appraisal, and expression of racial stereopytes (Gray et al., 2012; Garfinkel et al., 2014; Azevedo et al., 2017). By contrast, during the cardiac diastole, in which baroreceptor activity is minimal, detection of somatosensory stimuli is facilitated (Motyka et al., 2007; Al et al. 2018), and pre-motor responses to sensory stimulation are faster (Edwards et al., 2007). Thus, baroreceptor afferent activity modulates brain-body interactions during processing of sensory and painful stimuli, with a facilitatory role of maximum baroreceptor activity on threat-related processing.

In light of these findings, our results support that errors are salient events whose processing relies not only on proprioceptive and exteroceptive information, as shown previously (Ruiz et al., 2009; Orr and Carrasco, 2010; Boldt and Yeung, 2015; Ullsperger et al 2014), but also on implicit interoceptive cues, such as enhanced cardiovascular afferent signals. Ullsperger and colleagues (2010) have proposed that, following initial error detection by the pMFC, the conscious awareness of an error – as signalled by the PE component – engages the saliency network in addition to the executive network. Interestingly, the anterior insula (AI) and ACC are part of both networks (Seeley et al., 2007; Menon and Uddin, 2010). Moreover, the AI and ventral ACC are key centres for processing visceral information (Park et al., 2014; Barrett and Simons, 2015; Hassanpour et al., 2018). The AI has been linked to the generation of the PE and modulation of error awareness (Dhar et al., 2011). Additional correlational evidence coming from reaction-time tasks has shown that the PE is modulated by explicit interoception (heartbeat counting task, Sueyoshi et al., 2014). These previous studies thus favour the interpretation that interoceptive processing interacts with error monitoring mainly during the later stages, contributing to the conscious awareness of an error.

Crucially, we found that the error-correct ERP modulation by cardiovascular interoceptive signals occurred within 40-100ms, and thus preceded the PE component, which peaked around 150-250ms. This novel finding expands previous results (Dhar et al., 2011; Sueyoshi et al., 2014), by suggesting an earlier window in which visceral interoceptive information can modulate error processing, before conscious experience of the sensory consequences of an action. This finding

converges with the recent data on an earlier involvement of the AI – and potentially interoceptive processing – in error detection (Bastin et al., 2017). Thus early changes in cardiovascular information during error-monitoring processes could shape subsequent conscious evaluation of the error, thereby modifying ongoing performance. This interpretation is in agreement with a predictive account of interoception, whereby predictions about upcoming visceral sensations can drive behavioural and physiological responses to maintain homeostasis (Barrett and Simons, 2015; Seth and Friston, 2016). Predictive interoceptive processes are modulated by activity in the anterior insula (Barrett and Simons, 2015; Hassanpour et al., 2018), and can shape ongoing behaviour and (neuro)physiological states (Hassanpour et al., 2018; refs), including error-monitoring processes (Bastian et al., 2018).

The effect of the cardiac cycle on the error-correct ERP was linked to activity in the left inferior parietal lobe (IPL), a region implicated in human cardiac autonomic regulation and visceral processing (Lutz et al., 2009; Park et al., 2014). By contrast, source localization of the preERN and PE components revealed regions of the pMFC, such as the SMA, ACC and BA 9, which is consistent with the well-documented involvement of the pMFC in general error-monitoring (Dhar et al., 2011; Ullsperger et al., 2014). The IPL, along with the ventral ACC, AI and somatosensory areas, is part of the visceroneural network, which receives visceral information about bodily states (Lutz et al., 2009; Kleckner et al., 2017). Activity in this network might trigger changes in heart rate, such as HR deceleration following perceptual misses or response errors (Park et al., 2014; Bastin et al., 2017).

Here, we found a HR acceleration following pitch errors relative to correct keystrokes, which seems to stand in contrast with the post-error HR deceleration reported in previous studies (Hajcak et al., 2003; Wessel et al., 2011, Bastin et al., 2017). Significantly, however, a slowing down of the interbeat interval was found in error trials immediately preceding the key press. Moreover, the pattern of preceding HR changes at the single-trial level contained information predictive of whether an upcoming key press was an error or a correct event. The HR deceleration and acceleration effects before and after error commission, respectively, were independent of the cardiac phase with which errors coincided. Behaviorally, however, we found that following errors in

the cardiac systole there was a significantly reduced slowing of tempo and keystroke velocity at +2K post-error. These results, therefore, suggest that the modulation of IPL activity by cardiac interoceptive signals during error processing might be associated with a tuning of the gain on anticipatory HR changes driving subsequent behavioral alterations following pitch errors.

Thus, by investigating performance during a highly-trained motor task, this study provides the first evidence that prediction of upcoming errors triggers not only anticipatory error-detection ERP components, such as the preERN (Ruiz et al., 2009), but also anticipatory changes in interoceptive states. HR changes triggered by errors have been taken as evidence for an influence of error-related interoceptive signals on subsequent perceptual processing (Lukowska et al., 2018). Phasic activity in the locus coeruleus–norepinephrine system could drive these cardiovascular changes in response to errors (Ullsperger et al., 2010; Lukowska et al., 2018). Our study extends the findings of Lukowska and colleagues (2018) to the anticipatory period, when predictive error-detection components can shape anticipatory HR responses, thereby influencing subsequent performance.

We propose that a larger anterior IPL-dependent neural response during cardiac systole might reflect enhanced processing of interoceptive cues contributing to error processing. The anticipatory changes in cardiovascular information (sudden HR increase in error trials before the key press) could provide a form of feedback in addition to the early error-detection signatures to influence ongoing performance, and adapt subsequent behaviour. The cardiac systole may amplify processing of these early interoceptive cues, thus facilitating error detection, thereby diminishing the window of integration over which evidence for an error could be accumulated. Consequently, the slowing of responses following the error in the systolic phase is less pronounced. Note that in our study, PES effects extended for six successive keystrokes – or three keystrokes when assessing pitch errors of similar pre-error temporal properties than correct key presses – until timing performance progressively returned to baseline levels, converging with previous studies (Ruiz et al., 2009; Maidhof et al., 2009; Palmer et al., 2012). In this context, re-establishing accurate timing following error commission might be crucial for skilled performance (Goebl and Palmer, 2013), which here was facilitated during systole. Our interpretation is consistent with new

evidence supporting that post-error adjustments can be considered as a manifestation of a general orienting reflex rather than goal-directed adaptation (Notebaert et al., 2009; Wessell et al., 2017). As such, facilitation of error processing during maximal baroreceptor activity might ameliorate orienting responses and post-error slowing.

In conclusion, this study provides a novel account of implicit cardiovascular interoceptive signals modulating neural and behavioral responses related with early error monitoring during skilled performance. Early modulation of error processing by bodily signals might be particularly relevant during performance of a highly-trained task (Kleber et al., 2013). The anticipatory nature of error detection was here reflected in the preERN component, which has been interpreted as an index of a forward control process (Wolpert et al., 1998) that predicts unwanted sensory consequences of ongoing movements in a highly-trained task (Ruiz et al., 2009 Maidhof et al., 2009, 2013). Early error prediction might in turn trigger anticipatory corrective adjustments (Ruiz et al., 2011; Palmer et al., 2012), as reflected here in the reduced loudness and slower tempo at the error and preceding keystrokes. Expanding these previous findings, our novel data provide evidence that changes in the internal bodily state – a slowing of the HR immediately before errors – can anticipate the consequences of upcoming actions and modulate cortical responses to interoceptive cues to facilitate error processing. In addition, the data suggest that prediction of the upcoming consequences of our actions rely on the integration of exteroceptive and interoceptive information, a process likely shaped by long-term training (Schirmer-Mokwa et al., 2015; Kleber et al., 2013).

A limitation of our study is that EEG and source localization do not allow the investigation of insular activity during the anticipation and processing of errors, which would be crucial to understand the mechanisms by which anticipatory interoceptive states drive early error processes. These are likely mediated by insular activity. In addition, we did not use individual MRI scans to inform source modelling, but a standard template anatomy, as validated elsewhere (Haufe et al., 2016). Accordingly the source localisation results should be interpreted with care and need to be replicated in future studies. Follow-up studies using combined MRI and EEG or magnetoencephalography to assess cardiovascular influences on error processing across different stages of training will be central to further our understanding of the impact of interoception in expert performance.

References

Al, E., Iliopoulos, F., Forschack, N., Nierhaus, T., Grund, M., Gaebler, M., Motyka, P., Nikulin, V., Villringer, A., 2018. Do Somatosensory Detection and Localization Vary Across The Cardiac Cycle? Poster session presented at the Mind Body and Brain Symposium in Berlin, Germany.

Allefeld, C., Görgen, K., Haynes, J.-D., 2016. Valid population inference for information-based imaging: From the second-level t -test to prevalence inference. NeuroImage 141, 378–392. https://doi.org/10.1016/j.neuroimage.2016.07.040

Amiez, C., Joseph, J.-P., Procyk, E., 2005. Anterior cingulate error-related activity is modulated by predicted reward. European Journal of Neuroscience 21, 3447–3452. https://doi.org/10.1111/j.1460-9568.2005.04170.x

Azevedo, R.T., Garfinkel, S.N., Critchley, H.D., Tsakiris, M., 2017. Cardiac afferent activity modulates the expression of racial stereotypes. Nature Communications 8, 13854. https://doi.org/10.1038/ncomms13854

Babo-Rebelo, M., Richter, C.G., Tallon-Baudry, C., 2016. Neural Responses to Heartbeats in the Default Network Encode the Self in Spontaneous Thoughts. The Journal of Neuroscience 36, 7829–7840. https://doi.org/10.1523/jneurosci.0262-16.2016

Babo-Rebelo, M., Wolpert, N., Adam, C., Hasboun, D., Tallon-Baudry, C., 2016. Is the cardiac monitoring function related to the self in both the default network and right anterior insula? Philosophical Transactions of the Royal Society B: Biological Sciences 371, 20160004. https://doi.org/10.1098/rstb.2016.0004

Barrett, L.F., Simmons, W.K., 2015. Interoceptive predictions in the brain. Nature Reviews Neuroscience 16, 419–429. https://doi.org/10.1038/nrn3950

Bastin, J., Deman, P., David, O., Gueguen, M., Benis, D., Minotti, L., Hoffman, D., Combrisson, E., Kujala, J., Perrone-Bertolotti, M., Kahane, P., Lachaux, J.-P., Jerbi, K., 2016. Direct

Recordings from Human Anterior Insula Reveal its Leading Role within the Error-Monitoring Network. Cerebral Cortex bhv352. https://doi.org/10.1093/cercor/bhv352

Benjamini, Y., Krieger, A.M., Yekutieli, D., 2006. Adaptive linear step-up procedures that control the false discovery rate. Biometrika 93, 491–507. https://doi.org/10.1093/biomet/93.3.491

Bennarroch, EE., 1997. Central autonomic network: Functional organization and clinical correlations. Futura Publishing Company; Armonk, NY.

Boldt, A., Yeung, N., 2015. Shared Neural Markers of Decision Confidence and Error Detection. Journal of Neuroscience 35, 3478–3484. https://doi.org/10.1523/jneurosci.0797-14.2015

Bonini, F., Burle, B., Liegeois-Chauvel, C., Regis, J., Chauvel, P., Vidal, F., 2014. Action Monitoring and Medial Frontal Cortex: Leading Role of Supplementary Motor Area. Science 343, 888–891. https://doi.org/10.1126/science.1247412

Button, K.S., Ioannidis, J.P., Mokrysz, C., Nosek, B.A., Flint, J., Robinson, E.S. and Munafò, M.R., 2013. Power failure: why small sample size undermines the reliability of neuroscience. Nature Reviews Neuroscience, 14(5), p.365.

Carter, C.S., 1998. Anterior Cingulate Cortex, Error Detection, and the Online Monitoring of Performance. Science 280, 747–749. https://doi.org/10.1126/science.280.5364.747

Cavanagh, J. F., Cohen, M. X., & Allen, J. J. 2009. Prelude to and resolution of an error: EEG phase synchrony reveals cognitive control dynamics during action monitoring. Journal of Neuroscience, 29(1), 98-105.

Chang CC, Lin CJ. 2011. LIBSVM: a library for support vector machines. ACM transactions on intelligent systems and technology (TIST) 2(3):27.

Combrisson, E., Jerbi, K., 2015. Exceeding chance level by chance: The caveat of theoretical chance levels in brain signal classification and statistical assessment of decoding accuracy. Journal of Neuroscience Methods 250, 126–136. https://doi.org/10.1016/j.jneumeth.2015.01.010

Craig, A.D., 2009. How do you feel--now? The anterior insula and human awareness. Nature reviews neuroscience, 10(1).

Critchley, H.D., 2005. Neural mechanisms of autonomic, affective, and cognitive integration. The Journal of Comparative Neurology 493, 154–166. https://doi.org/10.1002/cne.20749

Critchley, H.D., Harrison, N.A., 2013. Visceral Influences on Brain and Behavior. Neuron 77, 624–638. https://doi.org/10.1016/j.neuron.2013.02.008

Delorme, A., Makeig, S., 2004. EEGLAB: an open source toolbox for analysis of single-trial EEG dynamics including independent component analysis. Journal of Neuroscience Methods 134, 9–21. https://doi.org/10.1016/j.jneumeth.2003.10.009

Dhar, M., Wiersema, J.R., Pourtois, G., 2011. Cascade of Neural Events Leading from Error Commission to Subsequent Awareness Revealed Using EEG Source Imaging. PLoS ONE 6, e19578. https://doi.org/10.1371/journal.pone.0019578

Duda, R.O., Hart, P.E. and Stork, D.G., 2012. Pattern classification. John Wiley & Sons. Journal of Classification 24, 305–307. https://doi.org/10.1007/s00357-007-0015-9

Edwards, L., Ring, C., McIntyre, D., Carroll, D. and Martin, U., 2007. Psychomotor speed in hypertension: Effects of reaction time components, stimulus modality, and phase of the cardiac cycle. Psychophysiology, 44(3), 459-468.

Fadel, P.J., Ogoh, S., Keller, D.M., Raven, P.B., 2003. Recent Insights into Carotid Baroreflex Function in Humans Using the Variable Pressure Neck Chamber. Experimental Physiology 88, 671–680. https://doi.org/10.1113/eph8802650

Falkenstein, M., Hoormann, J., Christ, S., Hohnsbein, J., 2000. ERP components on reaction errors and their functional significance: a tutorial. Biological Psychology 51, 87–107. https://doi.org/10.1016/s0301-0511(99)00031-9

Fiacconi, C.M., Peter, E.L., Owais, S., Köhler, S., 2016. Knowing by heart: Visceral feedback shapes recognition memory judgments. Journal of Experimental Psychology: General 145, 559–572. https://doi.org/10.1037/xge0000164

Fuchs, M., Kastner, J., Wagner, M., Hawes, S., Ebersole, J.S., 2002. A standardized boundary element method volume conductor model. Clinical Neurophysiology 113, 702–712. https://doi.org/10.1016/s1388-2457(02)00030-5

Garfinkel, S.N., Critchley, H.D., 2016. Threat and the Body: How the Heart Supports Fear Processing. Trends in Cognitive Sciences 20, 34–46. https://doi.org/10.1016/j.tics.2015.10.005

Garfinkel, S.N., Minati, L., Gray, M.A., Seth, A.K., Dolan, R.J., Critchley, H.D., 2014. Fear from the Heart: Sensitivity to Fear Stimuli Depends on Individual Heartbeats. Journal of Neuroscience 34, 6573–6582. https://doi.org/10.1523/jneurosci.3507-13.2014

Gehring, W.J., Goss, B., Coles, M.G.H., Meyer, D.E., Donchin, E., 1993. A Neural System for Error Detection and Compensation. Psychological Science 4, 385–390. https://doi.org/10.1111/j.1467-9280.1993.tb00586.x

Gianaros, P.J., Van der Veen, F.M. and Jennings, J.R., 2004. Regional cerebral blood flow correlates with heart period and high-frequency heart period variability during working-memory tasks: Implications for the cortical and subcortical regulation of cardiac autonomic activity. Psychophysiology, 41(4), 521-530.

Goebl, W., Palmer, C., 2013. Temporal Control and Hand Movement Efficiency in Skilled Music Performance. PLoS ONE 8, e50901. https://doi.org/10.1371/journal.pone.0050901

Permutation, Parametric and Bootstrap Tests of Hypotheses, 2005. , Springer Series in Statistics. Springer-Verlag. https://doi.org/10.1007/b138696

Grandchamp, R., Delorme, A., 2011. Single-Trial Normalization for Event-Related Spectral Decomposition Reduces Sensitivity to Noisy Trials. Frontiers in Psychology 2. https://doi.org/10.3389/fpsyg.2011.00236

Gray, M.A., Beacher, F.D., Minati, L., Nagai, Y., Kemp, A.H., Harrison, N.A., Critchley, H.D., 2012. Emotional appraisal is influenced by cardiac afferent information. Emotion 12, 180–191. https://doi.org/10.1037/a0025083

Grissom, R.J., 2014. Effect Sizes for Research. Routledge. https://doi.org/10.4324/9781410612915

Hajcak, G., McDonald, N., Simons, R.F., 2003. To err is autonomic: Error-related brain potentials, ANS activity, and post-error compensatory behavior. Psychophysiology 40, 895–903. https://doi.org/10.1111/1469-8986.00107

Hassanpour, M.S., Simmons, W.K., Feinstein, J.S., Luo, Q., Lapidus, R.C., Bodurka, J., Paulus, M.P. and Khalsa, S.S., 2018. The insular cortex dynamically maps changes in cardiorespiratory interoception. Neuropsychopharmacology, 43(2), 426.

Haufe, S., Ewald, A., 2016. A Simulation Framework for Benchmarking EEG-Based Brain Connectivity Estimation Methodologies. Brain Topography. https://doi.org/10.1007/s10548-016-0498-y

Haxby, J.V., 2001. Distributed and Overlapping Representations of Faces and Objects in Ventral Temporal Cortex. Science 293, 2425–2430. https://doi.org/10.1126/science.1063736

Herrmann, M.J., Römmler, J., Ehlis, A.-C., Heidrich, A., Fallgatter, A.J., 2004. Source localization (LORETA) of the error-related-negativity (ERN/Ne) and positivity (Pe). Cognitive Brain Research 20, 294–299. https://doi.org/10.1016/j.cogbrainres.2004.02.013

Kiehl, K.A., Liddle, P.F., Hopfinger, J.B., 2000. Error processing and the rostral anterior cingulate: An event-related fMRI study. Psychophysiology 37, 216–223. https://doi.org/10.1111/1469-8986.3720216

Kleber, B., Zeitouni, A.G., Friberg, A., Zatorre, R.J., 2013. Experience-Dependent Modulation of Feedback Integration during Singing: Role of the Right Anterior Insula. Journal of Neuroscience 33, 6070–6080. https://doi.org/10.1523/jneurosci.4418-12.2013

Kleckner, I.R., Zhang, J., Touroutoglou, A., Chanes, L., Xia, C., Simmons, W.K., Quigley, K.S., Dickerson, B.C., Feldman Barrett, L., 2017. Evidence for a large-scale brain system supporting allostasis and interoception in humans. Nature Human Behaviour 1, 69. https://doi.org/10.1038/s41562-017-0069

Luft, C.D.B., Bhattacharya, J., 2015. Aroused with heart: Modulation of heartbeat evoked potential by arousal induction and its oscillatory correlates. Scientific Reports 5. https://doi.org/10.1038/srep15717

Łukowska, M., Sznajder, M., Wierzchoń, M., 2018. Error-related cardiac response as information for visibility judgements. Scientific Reports 8. https://doi.org/10.1038/s41598-018-19144-0

Lutz, A., Greischar, L.L., Perlman, D.M., Davidson, R.J., 2009. BOLD signal in insula is differentially related to cardiac function during compassion meditation in experts vs. novices. NeuroImage 47, 1038–1046. https://doi.org/10.1016/j.neuroimage.2009.04.081

Maidhof, C., 2013. Error monitoring in musicians. Frontiers in Human Neuroscience 7. https://doi.org/10.3389/fnhum.2013.00401

Maidhof, C., Rieger, M., Prinz, W., Koelsch, S., 2009. Nobody Is Perfect: ERP Effects Prior to Performance Errors in Musicians Indicate Fast Monitoring Processes. PLoS ONE 4, e5032. https://doi.org/10.1371/journal.pone.0005032

Maris, E., Oostenveld, R., 2007. Nonparametric statistical testing of EEG- and MEG-data. Journal of Neuroscience Methods 164, 177–190. https://doi.org/10.1016/j.jneumeth.2007.03.024

Mazziotta, J., Toga, A., Evans, A., Fox, P., Lancaster, J., Zilles, K., Woods, R., Paus, T., Simpson, G., Pike, B., Holmes, C., Collins, L., Thompson, P., MacDonald, D., Iacoboni, M., Schormann, T., Amunts, K., Palomero-Gallagher, N., Geyer, S., Parsons, L., Narr, K.,

Kabani, N., Goualher, G.L., Boomsma, D., Cannon, T., Kawashima, R., Mazoyer, B., 2001. A probabilistic atlas and reference system for the human brain: International Consortium for Brain Mapping (ICBM). Philosophical Transactions of the Royal Society B: Biological Sciences 356, 1293–1322. https://doi.org/10.1098/rstb.2001.0915

Menon, V., Adleman, N.E., White, C.D., Glover, G.H., Reiss, A.L., 2001. Error-related brain activation during a Go/NoGo response inhibition task. Human Brain Mapping 12, 131–143. https://doi.org/10.1002/1097-0193(200103)12:3<131::aid-hbm1010>3.0.co;2-c

Menon, V., Uddin, L.Q., 2010. Saliency, switching, attention and control: a network model of insula function. Brain Structure and Function 214, 655–667. https://doi.org/10.1007/s00429-010-0262-0

Miller, E.K., 2000. The prefrontal cortex and cognitive control. Nat. Rev. Neurosci. 1, 59–65.

Miltner, W.H.R., Lemke, U., Weiss, T., Holroyd, C., Scheffers, M.K., Coles, M.G.H., 2003. Implementation of error-processing in the human anterior cingulate cortex: a source analysis of the magnetic equivalent of the error-related negativity. Biological Psychology 64, 157–166. https://doi.org/10.1016/s0301-0511(03)00107-8

Moller, J., Jansma, B.M., Rodriguez-Fornells, A., Munte, T.F., 2006. What the Brain Does before the Tongue Slips. Cerebral Cortex 17, 1173–1178. https://doi.org/10.1093/cercor/bhl028

Motyka, P., Grund, M., Forschack, N., Villringer, A., Gaebler, M., 2017. Conscious somatosensory perception varies across the cardiac cycle. Poster session presented at 21th Annual meeting of Association for the Scientific Study of Consciousness in Beijing, China.

Nakahara, H., Furuya, S., Obata, S., Masuko, T., Kinoshita, H., 2009. Emotion-related Changes in Heart Rate and Its Variability during Performance and Perception of Music. Annals of the New York Academy of Sciences 1169, 359–362. https://doi.org/10.1111/j.1749-6632.2009.04788.x

Notebaert, W., Houtman, F., Opstal, F.V., Gevers, W., Fias, W., Verguts, T., 2009. Post-error slowing: An orienting account. Cognition 111, 275–279. https://doi.org/10.1016/j.cognition.2009.02.002

Oostenveld, R., Fries, P., Maris, E., Schoffelen, J.-M., 2011. FieldTrip: Open Source Software for Advanced Analysis of MEG, EEG, and Invasive Electrophysiological Data. Computational Intelligence and Neuroscience 2011, 1–9. https://doi.org/10.1155/2011/156869

Open Science Collaboration, 2015. Estimating the reproducibility of psychological science. Science, 349(6251), p.aac4716.

Orr, J.M., Carrasco, M., 2011. The Role of the Error Positivity in the Conscious Perception of Errors. Journal of Neuroscience 31, 5891–5892. https://doi.org/10.1523/jneurosci.0279-11.2011

Palmer, C., 2006. The nature of memory for music performance skills, in: Music, Motor Control and the Brain. Oxford University Press, pp. 39–54. https://doi.org/10.1093/acprof:oso/9780199298723.003.0003

Palmer, C., Mathias, B., Anderson, M., 2012. Sensorimotor mechanisms in music performance: actions that go partially wrong. Annals of the New York Academy of Sciences 1252, 185–191. https://doi.org/10.1111/j.1749-6632.2011.06427.x

Park, H.-D., Bernasconi, F., Bello-Ruiz, J., Pfeiffer, C., Salomon, R., Blanke, O., 2016. Transient Modulations of Neural Responses to Heartbeats Covary with Bodily Self-Consciousness. Journal of Neuroscience 36, 8453–8460. https://doi.org/10.1523/jneurosci.0311-16.2016

Park, H.-D., Correia, S., Ducorps, A., Tallon-Baudry, C., 2014. Spontaneous fluctuations in neural responses to heartbeats predict visual detection. Nature Neuroscience 17, 612–618. https://doi.org/10.1038/nn.3671

Pollatos, O., Schandry, R., 2004. Accuracy of heartbeat perception is reflected in the amplitude of the heartbeat-evoked brain potential. Psychophysiology 41, 476–482. https://doi.org/10.1111/1469-8986.2004.00170.x

Ruiz, M.H., Jabusch, H.-C., Altenmüller, E., 2009. Detecting Wrong Notes in Advance: Neuronal Correlates of Error Monitoring in Pianists. Cerebral Cortex 19, 2625–2639. https://doi.org/10.1093/cercor/bhp021

Ruiz, M.H., Rusconi, M., Brücke, C., Haynes, J.-D., Schönecker, T., Kühn, A.A., 2014. Encoding of sequence boundaries in the subthalamic nucleus of patients with Parkinson's disease. Brain 137, 2715–2730. https://doi.org/10.1093/brain/awu191

Ruiz, M.H., Strübing, F., Jabusch, H.-C., Altenmüller, E., 2011. EEG oscillatory patterns are associated with error prediction during music performance and are altered in musician's dystonia. NeuroImage 55, 1791–1803. https://doi.org/10.1016/j.neuroimage.2010.12.050

Schellenberg, E.G., W. Weiss, M., 2013. Music and Cognitive Abilities, in: The Psychology of Music. Elsevier, pp. 499–550. https://doi.org/10.1016/b978-0-12-381460-9.00012-2

Schirmer-Mokwa, K.L., Fard, P.R., Zamorano, A.M., Finkel, S., Birbaumer, N., Kleber, B.A., 2015. Evidence for Enhanced Interoceptive Accuracy in Professional Musicians. Frontiers in Behavioral Neuroscience 9. https://doi.org/10.3389/fnbeh.2015.00349

Seeley, W.W., Menon, V., Schatzberg, A.F., Keller, J., Glover, G.H., Kenna, H., Reiss, A.L., Greicius, M.D., 2007. Dissociable Intrinsic Connectivity Networks for Salience Processing and Executive Control. Journal of Neuroscience 27, 2349–2356. https://doi.org/10.1523/jneurosci.5587-06.2007

Seth, A. K., & Friston, K. J. 2016. Active interoceptive inference and the emotional brain. Phil. Trans. R. Soc. B, 371(1708), 20160007.

Steinhauser, M., Yeung, N., 2010. Decision Processes in Human Performance Monitoring. Journal of Neuroscience 30, 15643–15653. https://doi.org/10.1523/jneurosci.1899-10.2010

Stevens, F.L., Hurley, R.A., Taber, K.H., 2011. Anterior Cingulate Cortex: Unique Role in Cognition and Emotion. The Journal of Neuropsychiatry and Clinical Neurosciences 23, 121–125. https://doi.org/10.1176/jnp.23.2.jnp121

Sueyoshi, T., Sugimoto, F., Katayama, J. 'ichi, Fukushima, H., 2014. Neural correlates of error processing reflect individual differences in interoceptive sensitivity. International Journal of Psychophysiology 94, 278–286. https://doi.org/10.1016/j.ijpsycho.2014.10.001

Ullsperger, M., Danielmeier, C., Jocham, G., 2014. Neurophysiology of Performance Monitoring and Adaptive Behavior. Physiological Reviews 94, 35–79. https://doi.org/10.1152/physrev.00041.2012

Ullsperger, M., Harsay, H.A., Wessel, J.R., Ridderinkhof, K.R., 2010. Conscious perception of errors and its relation to the anterior insula. Brain Structure and Function 214, 629–643. https://doi.org/10.1007/s00429-010-0261-1

Vázquez-Seisdedos, C.R., Neto, J., Marañón Reyes, E.J., Klautau, A., Limão de Oliveira, R.C., 2011. New approach for T-wave end detection on electrocardiogram: Performance in noisy conditions. BioMedical Engineering OnLine 10, 77. https://doi.org/10.1186/1475-925x-10-77

Vorwerk, J., Oostenveld, R., Piastra, M.C., Magyari, L. and Wolters, C.H., 2018. The FieldTrip-SimBio pipeline for EEG forward solutions. Biomedical engineering online, 17(1), 37.

Weisz, J., & Adam, G. 1996. The influence of cardiac phase on reaction time depending on heart period length and on stimulus and response laterality. Psychobiology 24, 169–175.

Wessel, J.R., 2017. An adaptive orienting theory of error processing. Psychophysiology 55, e13041. https://doi.org/10.1111/psyp.13041

Wessel, J.R., Danielmeier, C., Ullsperger, M., 2011. Error Awareness Revisited: Accumulation of Multimodal Evidence from Central and Autonomic Nervous Systems. Journal of Cognitive Neuroscience 23, 3021–3036. https://doi.org/10.1162/jocn.2011.21635

Wittfoth, M., Schardt, D. M., Fahle, M., & Herrmann, M. 2009. How the brain resolves high conflict situations: double conflict involvement of dorsolateral prefrontal cortex. Neuroimage, 44(3), 1201-1209.

Wolpert, D.M., Kawato, M., 1998. Multiple paired forward and inverse models for motor control. Neural Networks 11, 1317–1329. https://doi.org/10.1016/s0893-6080(98)00066-5

Figures

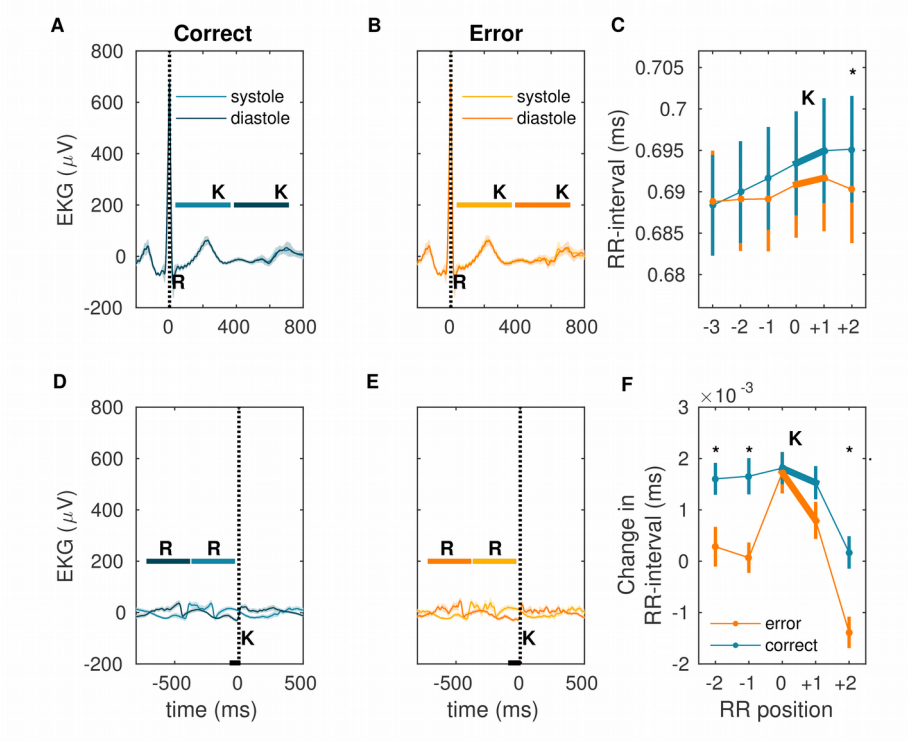

Figure 1. **Electrocardiogram (ECG)**. Grand-average across subjects. Shaded areas show ± 1 s.e.m. around the mean. **(A)** Analysis of ECG locked to the R-peak for correct notes falling within the systolic (light blue) or diastolic (dark blue) phase of the cardiac cycle revealed no significant differences ($p > 0.05$). The blue horizontal likes denoted by "K" highlight the temporal interval in which the keystroke fell for each phase of the cardiac cycle. The interval was 50-350 ms for the systolic and from 400 ms until the next R-peak (693, s.e.m. 15, ms on average) for the diastolic phase. The vertical line denoted by 'R' indicates the onset of the R peak. **(B)** Same as (A) but in error trials. No significant differences between the R-peak-locked ECG in bin1 (systole, light orange) and bin2 (diastole, dark orange) trials was found ($p > 0.05$). **(C)** Heart-rate changes

around pitch errors (in orange) compared to correct key presses (in blue) measured as RR-interval (ms) and shown as mean and s.e.m. bars. The thicker line segments from RR-interval position 0 to 1 highlight the time interval in which the error or correct keys were pressed (also denoted by “K”). The RR-interval differed significantly between error and correct key presses exclusively at position +2K following keystrokes, due to a relative faster heart rate following errors ($p < 0.05$, FDR-corrected, $PS_{dep} = 0.94$). **(D)** ECG locked to the keystroke following R-peaks and separately for bins 1 and 2 in correct trials. Time 0 ms marks the correct note onset, denoted by the vertical line (labeled “K”). The shifted ECG waveforms in bin1 and bin2 were significantly different within [-53, -8] ms (black bottom line; $p < 0.05$, FDR-corrected; $PS_{dep} = 0.875$). The horizontal lines in light and dark blue denoted by 'R' indicate the temporal intervals of the R-peak preceding the keystrokes in each bin. **(E)** Same as (D) but for error trials. The shifted ECG waveforms locked to pitch errors differed significantly between bin1 and bin2 trials also in the pre-keystroke interval, similarly to the results in correct trials, within [-74, -18] ms ($p < 0.05$, FDR-corrected; $PS_{dep} = 0.818$). **(F)** Same as (C) but for differences between consecutive RR-intervals (e.g. RR-interval at position 0, before the keystroke, relative to the previous RR-interval). The RR-interval change prior to error keystrokes was smaller than in error trials (-2, -1, positions) as well as following the keystrokes at the +2 RR-interval position ($p < 0.05$, FDR-corrected; PS_{dep} in range 0.76 – 0.85). The pronounced drop in RR-interval change following errors relative to correct notes indicated that pianists’ heart rate speeded up after a pitch error, yet slowed down prior to error commision (positive change at position 0 relative to the previous one -1 in the RR-interval ($p < 0.05$, FDR-corrected; $PS_{dep} = 0.84$).

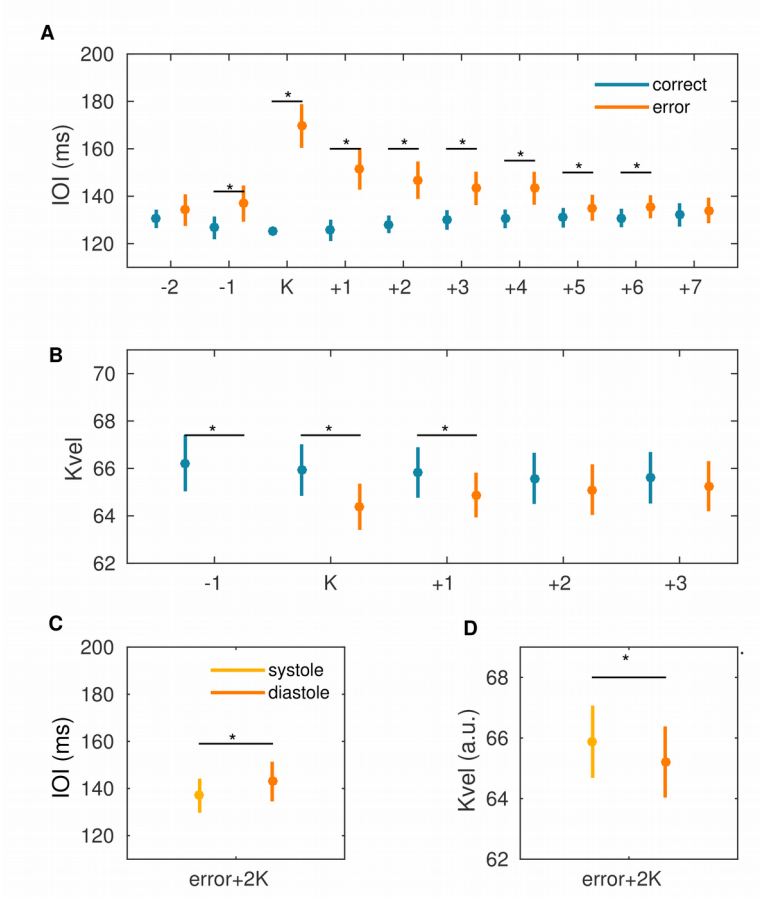

Figure 2. **Behavioral data.** Data are presented as mean and s.e.m. bars. **(A)** Mean inter-onset-interval, IOI (ms), across different keystroke positions relative to the central target keystroke (pitch errors, in orange; correct note, in blue), denoted by "K". The mean timing of keystrokes before and after pitch errors was significantly slower than the average tempo of keystrokes surrounding correct key presses at the same position (positions -1, +1, +2, +3, +4, +5, +6; $p < 0.05$, FDR-corrected; PS_{dep} in range 0.73-0.94; significant differences denoted by the horizontal black lines with an asterisk). Pitch errors were also slower than correct keystrokes ($p < 0.05$, FDR-corrected; PS_{dep} = 1). **(B)** The mean keystroke velocity, associated with the loudness, at pitch errors as well as preceding and following errors was significantly reduced compared to the keystroke velocity of correct notes at the same position (positions -1, central keystroke, +1; $p < 0.05$, FDR-corrected; Ps_{dep} was 0.94, 0.76, 0.59, respectively). **(C)** The slowing of performance timing at pitch errors and at +2K following errors was significantly smaller when the pitch errors coincided with the systolic

(light orange), relative to the diastole (dark orange), period of the cardiac cycle ($p < 0.05$, FDR-corrected; $PS_{dep} = 0.77$ and 0.69, respectively).

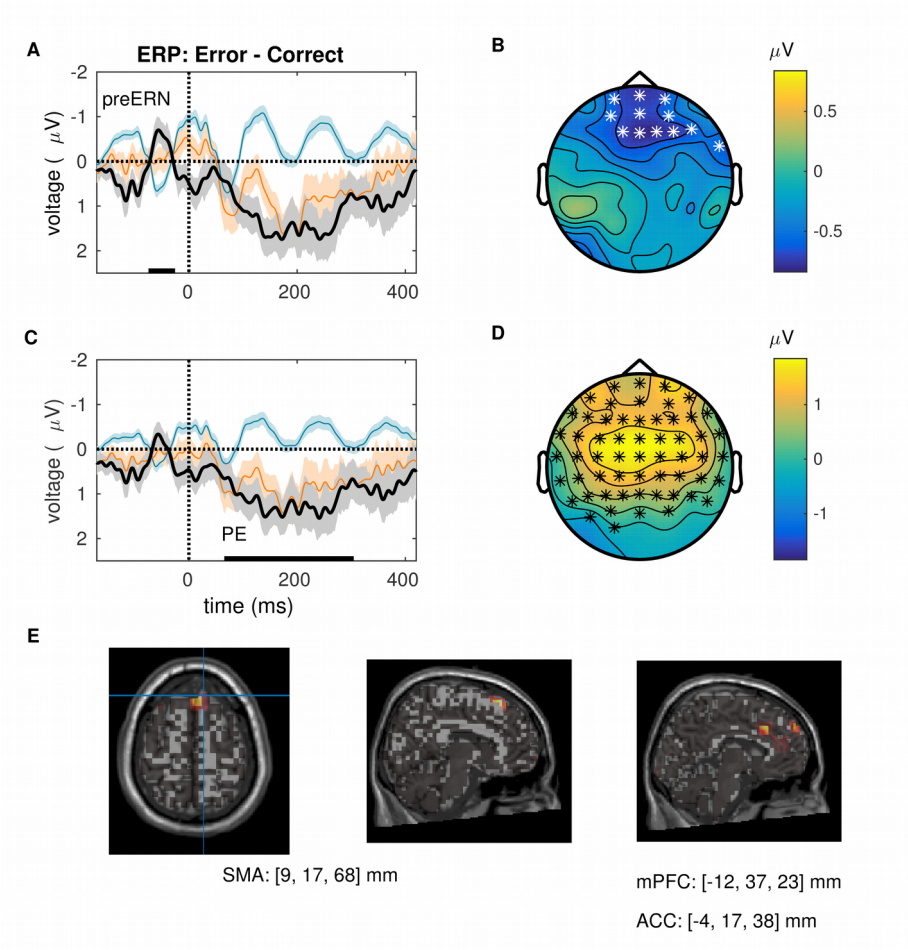

Figure 3. Neural signatures of error detection locked to keystrokes. (A). Note-onset event-related potentials (ERP) depicted at frontal electrodes for pitch errors (orange line), correct notes (blue line) and for the difference (errors minus correct notes, black line). The keystroke at time 0ms is denoted by the dashed line. Shaded areas show ± 1 s.e.m. around the mean. The electrodes selected for this representation belonged to the significant negative cluster depicted in panel (B). Note the negative deflection preceding error commission (pre-error-related negativity, preERN). Black bars at the bottom indicate time windows of significant differences in this cluster ($p = 0.0159$, cluster-based permutation test). **(B)** Scalp topography for the preERN component, corresponding to the significant negative cluster obtained within -70 to -30 ms prior to keystrokes ($p = 0.0159$, cluster permutation test, $p < 0.025$, two-sided test) for the error-correct note difference comparison. The white stars denote the electrodes belonging to the significant cluster.

(C) ERP waveforms locked to keystrokes as in (A), but here averaged across significant electrodes that were part of the significant positive cluster represented in (D). The black bar at the bottom denotes the significant slower positive modulation following errors relative to correct key presses (error positivity, PE). **(D)** Scalp topography for the PE component, associated with the significant positive cluster obtained within 80 to 300ms following erroneous relative to correct keystrokes ($p = 0.0199$, $p < 0.025$). The black stars denote the electrodes belonging to the significant cluster. **(E)** Significant neural sources of the preERN (similar results for the PE: minimum norm estimate, regularization parameter $\lambda = 0.1$). MNI coordinates for sources at SMA, BA 6 (left panel), ACC and BA 9 in the medial prefrontal cortex (middle and right panels) are provided below.

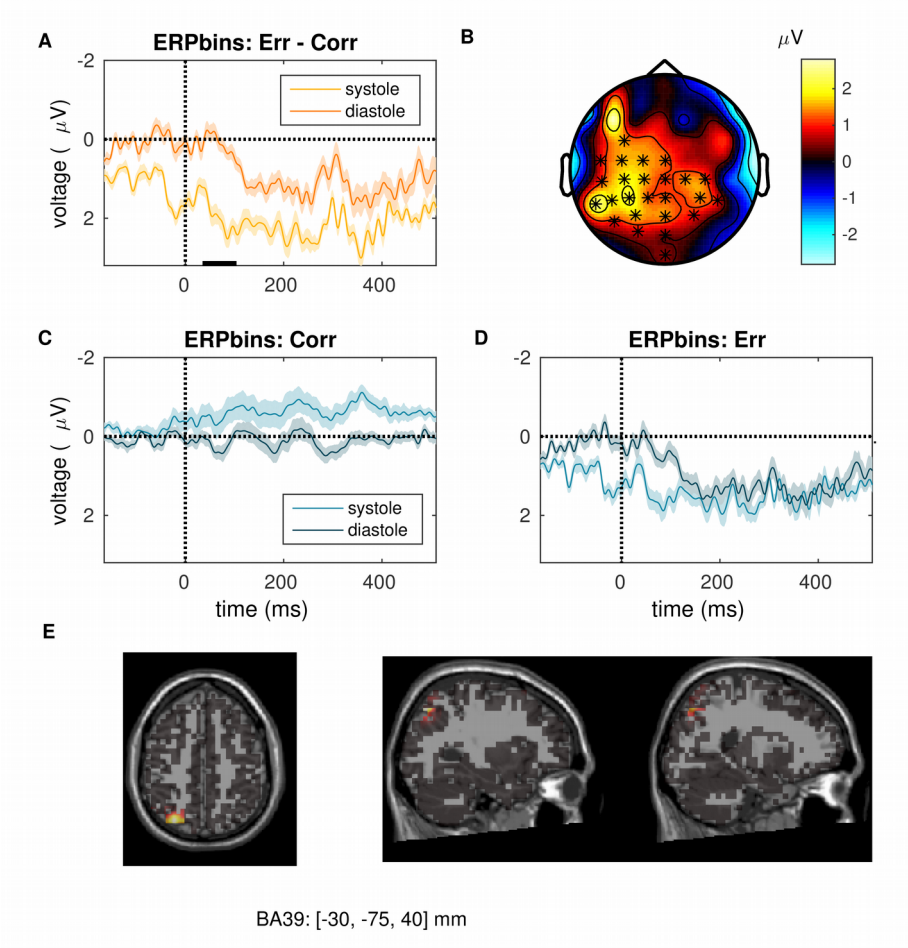

Figure 4. Influence of the cardiac cycle on the neural signatures of error detection locked to keystrokes. (A) Difference (error minus correct) event-related potentials (ERP) locked to keystrokes at time 0 ms (denoted by the vertical dashed line). The error-correct difference ERP is plotted separately for bin1 and bin2 trials, in which the keystroke coincided with the systolic (light

orange) or diastolic (dark orange) period of the cardiac cycle, respectively. The black bar at the bottom indicates the window of significant difference between the ERPs in the cardiac systolic and diastole periods (p = 0.021, two-sided cluster-based permutation test). The waveforms are averaged across electrodes pertaining to the significant cluster shown in panel (B). **(B)** Scalp topography for the significant cluster corresponding with the effect of the period of the cardiac cycle on the error-correct ERP waveforms locked to keystrokes. Keystrokes coinciding with the systolic relative to the diastolic period elicited a larger positive deflection in the error-correct ERP waveforms (p = 0.021, two-sided cluster-based permutation test). The black stars denote the electrodes belonging to the significant cluster. **(C)** ERP waveforms locked to correct keystrokes at systolic (light blue) and diastolic (dark blue) phases of the cardiac cycle. No significant difference was found between these two waveforms (p = 0.192). **(D)** Same as (C) but for pitch errors. No significant difference was found either (p = 0.281). **(E)** Significant neural source (minimum norm estimate, regularization parameter l = 0.1) for the difference between the error-correct ERP waveform in the cardiac systole and diastole. Standard MNI coordinates of the anatomical location in the left inferior parietal cortex (Brodmann area 39) is shown below.

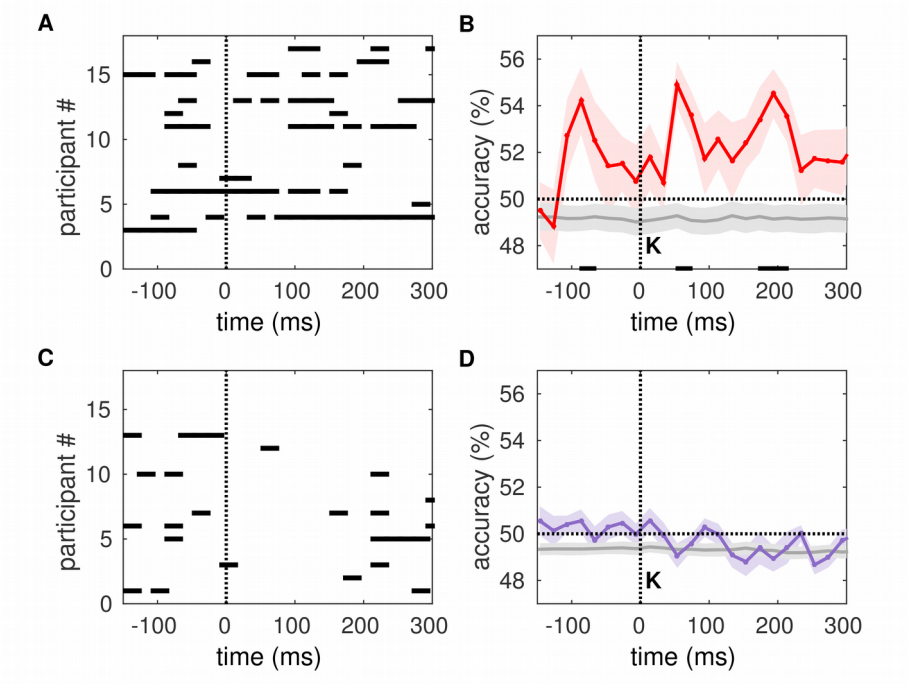

Figure 5. Multivariate pattern classification analysis (MVPA). MVPA for two classes of events: EEG trials locked to keystrokes in the cardiac systole and diastole. **(A)** Time windows of significant

above-chance decoding accuracy in error trials for single-subject MVPA analysis are denoted by horizontal bars (permutation tests, $p < 0.05$, FDR-corrected after control of FDR at level $q = 0.05$). **(B)** Population decoding accuracy for error trials plotted as the mean across participants (red line) and s.e.m. (red shade). Gray solid line indicates the chance level (s.e.m. as shaded gray area) on the group level estimated with permutation tests. Significant windows of above-chance decoding accuracy are denoted by the bottom vertical lines ($p < 0.05$, FDR-corrected, $PS_{dep} = 0.970$). The keystroke at time 0ms is indicated by the vertical dashed line. **(C)** Same as (A) but in correct trials. Significant above-chance decoding accuracy on the single-subject level is denoted by the horizontal black likes (permutation tests, *$p < 0.05$, FDR-corrected*). **(D)** Population decoding accuracy for correct trials plotted as the mean across participants (purple line) and s.e.m. (purple shade). There was no significant decoding accuracy above chance level in error trials ($p > 0.05$). The chance level (gray line; s.e.m shaded gray area) was estimated using permutation tests.

Table 1. Performance data in each condition expressed as mean (s.e.m.).

Percentage of total pitch errors	3.7% (1%)
Percentage of isolated pitch errors	1.4% (0.2%)
Number of total pitch errors	400 (90)
Number of isolated errors	153 (16)
Number of total notes played	10600 (380)
Mean IOI of correct pitch keystrokes (ms)	125 (0.1)
Mean IOI of isolated pitch errors (ms)	169 (8)
Overall loudness: Correct pitch	66 (1)
Overall loudness: Pitch errors	64 (1)
Mean IOI at +K following isolated pitch errors (ms)	149 (8)
Mean IOI at +2K following isolated pitch errors (ms)	147 (7)
Mean IOI at +3K following isolated pitch errors (ms)	143 (6)
Mean IOI at -K preceding isolated pitch errors (ms)	134 (6)
Mean IOI at -2K preceding isolated pitch errors (ms)	131 (6)